Journal of NeuroVirology (1997) 3, 387–400

http://www.jneurovirol.com

Review

The entry of antiviral and antiretroviral drugs into the central nervous system

Dennis R Groothuis[1,2,3] and Robert M Levy[3,4,5]

[1]Department of Neurology, Northwestern University Medical School, Evanston Hospital, Illinois 60201; [2]Department of Neurobiology and Physiology; [3]Northwestern University Institute for Neuroscience, Northwestern University, Evanston, Illinois 60208; [4]Department of Surgery (Neurosurgery); [5]Department of Physiology, Northwestern University Medical School, Chicago, Illinois, USA

The ability of antiviral and antiretroviral drugs to enter the brain is a critical issue in the treatment of many viral brain diseases, including HIV-related neurologic disease. Much of the literature concerning nucleoside analog entry into the nervous system focuses on drug levels in the cerebrospinal fluid (CSF), equating these with drug levels in the brain extracellular fluid (ECF) as though the two compartments intermix freely. We review the anatomic and physiologic aspects of drug entry into CSF and into brain ECF, as well as the exchange processes between these two compartments. In most instances drug concentrations in the CSF and ECF compartments bear little relationship to one another and using CSF concentrations to extrapolate brain ECF concentrations may significantly overestimate the latter. Accepted terminology and methodology for making measurements of blood–brain barrier function are discussed. Studies of brain uptake that express results as brain:plasma ratios, or that have used microdialysis, may overestimate the amount of drug reaching the brain. Using published data, we present an estimate of the time course of Zidovudine (AZT) concentrations in brain ECF and show that brain concentrations of AZT will likely be below that necessary to inhibit HIV-1 replication when AZT is administered systemically. Antiviral nucleosides and oligonucleotides appear to have limited entry into the brain when given systemically, which may hinder therapy of viral brain diseases, while some of the protease inhibitors may enter the brain more readily. Alternative methods for increasing antiviral and antiretroviral drug delivery to brain are discussed.

Keywords: antiretroviral; antisense; antiviral; blood–brain barrier; CSF; nucleoside; zidovudine

Introduction

The ability of antiviral drugs to enter the central nervous system (CNS) in therapeutic amounts is important for the therapy of many viral diseases, including AIDS. Not only must these agents reach the brain in sufficient concentrations to treat virally caused neurologic disease, but in AIDS the CNS viral reservoir must be adequately treated before systemic HIV therapy can be fully effective. Throughout the literature dealing with antiviral and antiretroviral therapy, statements about cerebrospinal fluid (CSF) production, the CSF space, and drug levels in the CSF are intermingled with those about the blood–brain barrier (BBB), the extracellular space of the brain (ECF), and drug levels in the ECF (Wang and Sawchuk, 1995; Cohn *et al*, 1996; Flexner and Hendrix, 1997). That the CSF and ECF compartments are freely interchangeable is a misconception. Measurements of CSF drug concentration are neither equivalent to nor reflect those in the brain extracellular fluid. This confusion first arose in a review article concerning nucleoside transport into the nervous system, which stated there was no barrier to movement of molecules between the ECF of the brain and the CSF (Spector and Eells, 1984). This conclusion was based upon a pharmacokinetic model of brain:CSF:plasma exchange in which ECF and CSF were presented as freely interchangeable (Figure 1) and the concentration of water-soluble molecules in CSF and ECF of

Correspondence: D Groothuis, 2650 Ridge Avenue, Evanston, Illinois, USA
Received 8 April 1997; revised 3 September 1997; accepted 21 October 1997

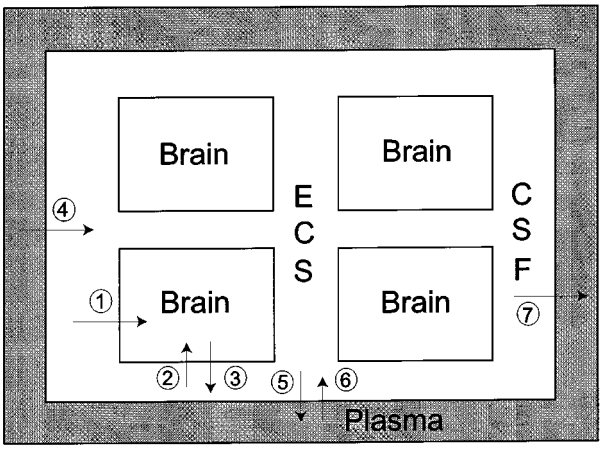

Figure 1 Model of interrelationships of plasma, CSF and brain extracellular space (ECS). This model is slightly modified from that of Spector *et al* (1977). Arrows 1 and 4 indicate active transport into brain and CSF, respectively. Arrows 2, 3, 5, and 6 indicate transport between compartments by simple diffusion. Arrow 7 indicates bulk flow of CSF into plasma. Note that no distinction is indicated between the ECS and CSF, nor are any barriers indicated.

brain were assumed to be identical (Spector *et al*, 1977). This assumption was never directly tested or confirmed. Nonetheless, this model of the equivalence of CSF and brain ECF was employed in subsequent studies of nucleoside transport into the brain (Spector, 1980, 1982, 1985a, b) and became widely adopted (Gallo, 1991). CSF and ECF are now frequently used almost interchangeably in articles about nucleoside analog transport into the nervous system. Unfortunately, this model does not accurately reflect the differences between CSF and brain ECF physiology and may have led to overstatements about the ability of antiviral and antiretroviral drugs to enter the nervous system.

It is important to identify the four separate compartments involved in the drug exchange process of the nervous system: (1) blood, (2) cerebrospinal fluid (CSF), (3) brain extracellular fluid (ECF), and (4) intracellular fluid of brain cells (ICF). A fifth compartment, representing an intracellular target such as nuclear DNA, may also be considered for many of these compounds. None of these compartments are interchangeable or freely intermixed. We will briefly review the general anatomy and physiology of exchange across the blood–brain barrier (blood⇄ECF), CSF formation (blood⇄CSF), and exchange between ECF and CSF (ECF⇄CSF), as well as experimental methods that have been used to study drug entry into these compartments. We will discuss the relationships between solute (drug) concentration in the CSF and the ECF and show that for most, the concentration in one compartment does not accurately reflect the concentration in the other. We will discuss whether the rate of brain entry of the different classes of antiviral and antiretroviral drugs is likely to result in therapeutic tissue levels. Finally, we will discuss methods that may be useful in the future to enhance antiviral drug delivery into the CNS.

Anatomy and physiology of drug delivery to the brain

The blood brain barrier (BBB) The BBB is deceptively simple. Except for geographically restricted areas such as the hypothalamus and area postrema, brain capillaries are continuous, unfenestrated, and are joined together by tight interendothelial junctions (Figure 2a). This two membrane, diffusion-limited system is called the blood–brain barrier (BBB) and has been well characterized (Rapoport, 1976; Bradbury, 1979, 1992; Davson and Segal, 1996). A few nutrients (such as glucose) have transport systems across the BBB, although the capacity and rate of the transport systems can vary widely: Betz *et al* (1994) estimated the transport rate for glucose as 700 nmol/g/min, while that for nucleosides was 0.006 nmol/g/min, i.e., 100 000-fold lower. In contrast to solutes with transport systems, most therapeutic drugs, including most of the nucleoside analogs, protease inhibitors, non-nucleoside reverse transcriptase inhibitors, and oligonucleotides, cross the BBB passively at a rate that can be related to the solute's water:lipid solubility, diffusion constant, and/or molecular size.

Since BBB passage of most antiviral drugs is passive (i.e. diffusion-limited) and because the transfer range is so large, the methodology used to measure brain uptake and the terminology used to express the blood-to-brain transfer process are critical to understanding the antiviral and antiretroviral drug delivery process. Many different experimental methods and expressions have been used (Table 1). One of the most direct, and most widely used, approaches has been to express results as ratios of 'brain' to plasma concentration. When measurements of drug concentration are made from a volume of brain tissue, the sample contains drug in *both* the blood compartment *and* and extracellular space compartment. The relative drug concentration in these compartments varies with time (Budinger and Huesman, 1985):

$$C_m(t) = Ci(t) + V_p C_p(t) \qquad 1$$

where $C_m(t)$ represents the measured concentration in a brain sample at time t, Ci(t) is the brain concentration (extracellular+intracellular), V_p is the fraction of tissue occupied by plasma, and $C_p(t)$ is freely exchangeable plasma concentration. Simple ratios of brain to plasma concentration will overestimate the amount of drug in the brain by the amount V_pC_p. The magnitude of the overestimate will depend upon both the permeability of the drug being studied with respect to the brain capillaries

and the time at which the measurement is made. This is illustrated in Figure 3 by time-activity curves for two water-soluble compounds, modeled using Equation 7 below, with permeabilities similar to AZT and an oligonucleotide. A plasma half life of 60 min was used in a simple two compartment model, the compounds were assumed to distribute passively across the BBB, have linear kinetics, and not be metabolized by brain. Using ratios of brain to plasma concentration to express brain uptake will produce a time-dependent error that increases in magnitude as water solubility of the drug increases. Consequently, using measurements of brain drug concentration that have not been corrected for the vascular space component (V_pC_p) to express brain uptake is less than desirable.

Using estimates of the brain plasma volume fraction from the literature to correct C_m for the vascular space component (V_pC_p) will improve the accuracy of brain:plasma ratios, but does not necessarily solve the problem since published estimates of V_p vary. Direct measurements of cerebral blood volume (V_v, where $V_v=V_{rbc}+V_p$) indicate a species difference: blood volume in rats varies between 5 and 15 μl/g (Cremer and Seville, 1983; Nakagawa *et al*, 1988), while in dogs V_v varies between 30 and 150 μl/g (Archer *et al*, 1987; Artru, 1987; Levin and Gilboe, 1970) and in man V_v is approximately 30–50 μl/g (Kuhl *et al*, 1980; Sakai *et al*, 1985). Because of the species differences, regional variability, and because V_v varies with type of anesthesia (Archer *et al*, 1987), it is wise to

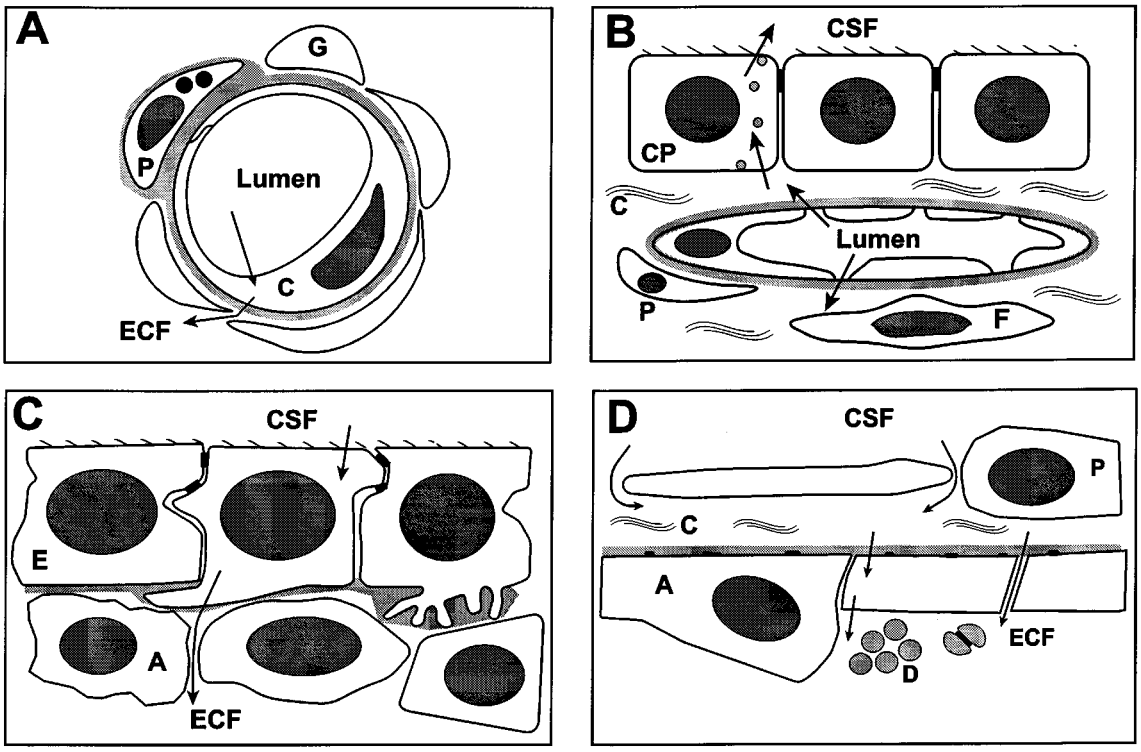

Figure 2 Anatomy of brain:blood:CSF interfaces. (**a**) Brain capillary: site of the blood–brain barrier. Brain capillaries (C) are continuous with tight interendothelial junctions, and are surrounded by a basement membrane (light gray), which may also envelope pericytes (P). Glial foot processes (G) abut on the basement membrane. Blood-borne solutes must cross from the lumen to the brain extracellular fluid (ECF). Passively distributed solutes must diffuse across both luminal and abluminal capillary membranes (indicated by arrows). (**b**) Choroid plexus. A diagrammatic section of one side of the choroid plexus is shown. Choroid plexus capillaries are fenestrated and surrounded by basement membrane, which many also envelope pericytes (P). Solutes leaving the choroid capillary initially reside in the extracellular space of the choroid plexus, which also contains fibroblasts (F) and collagen (C), not found in brain. The solute must then traverse the choroidal epithelium (CP), the apices of which are joined by tight interendothelial junctions, before entering the CSF. The choroidal epithelium is ciliated. (**c**) Lining of the ventricular surfaces. For the most part, the ventricular surfaces are lined by ciliated ependymal cells (E), although these vary in structure throughout the ventricular system. Ependymal cells may be joined by tight junctions in some areas, with a discontinuous junctional apparatus in other areas. A basement membrane (light gray) is found immediately beneath the ependymal cells and astrocytic processes (A) are generally underneath the basement membrane. Solutes in the CSF may be required to traverse the ependymal cells in some areas or may enter brain ECF between ependymal cells in other areas. (**d**) Lining of the brain surfaces. Once CSF leaves the ventricular system, it percolates through the subarachnoid space, which contains collagen bundles (C) and the pia mater (P) and comes into contact with the glia limitans of the brain surface. The glia limitans consists of flattened astrocytic processes (A) that are not joined by intercellular junctions. A basement membrane (light gray) covers the glia limitans and is held to it by junctional apparatuses. CSF may exchange with the brain ECF by traversing the glial processes or passing between them. In the cerebral cortex, dendrites (D) and synapses may be found immediately below the glia limitans.

Table 1 Commonly used expressions to describe brain uptake

Expression	*Symbol*	*Units*	*Comment*
Brain:Plasma ratio	None	None	Time dependent; may be corrected or uncorrected for amount in tissue vessels
Equilibrium rate constant	k	Reciprocal time	Describes time course of a process
Equilibrium half-time	$t_{1/2}$	Time	Functional expression; dependent upon equilibrium volume and efflux constant
Brain uptake index	BUI	None	Relative fractional loss from blood during single capillary passage
Extraction fraction	E	None	Fractional loss from blood during single capillary passage
Permeability	P	cm/sec	Physical constant
Permeability surface area product	PA or PS	cm^3/g/sec or ml/g/min	Functional expression per unit tissue weight, units of clearance
Transfer constant	K	ml/g/min	Functional expression per unit tissue weight, units of clearance

These are expressions that have been used to describe the blood-to-brain uptake proces with antiviral and antiretroviral drugs. The last four expressions (E, P, PS, and K) can be mathematically interrelated (see Equations 3–5).

include a vascular space marker or to use analytic methods that are independent of measures of V_p or V_v (discussed below).

A semiquantitative term for expressing the rate of brain entry is the Brain Uptake Index (BUI), which expresses the brain extraction of a solute *relative* to that of a highly diffusible substance, usually water or butanol (Oldendorf, 1970). The BUI produces an expression of brain influx as a percentage of the uptake of the reference compound. BUI values less than 3% are generally considered unreliable because brain solute counts are near background values (Cornford and Olendorf, 1975), but are nonetheless indicative of limited BBB passage.

However, to gain a more complete understanding about the blood–brain–CSF exchange process, appropriate physiological models must be used along with appropriate pharmacokinetic methods for analyzing the data. Fenstermacher has summarized methods to measure blood-to-brain transfer (Fenstermacher *et al*, 1981; Fenstermacher, 1989), for which several different expressions are in common use (Table 1). Frequently, the time component of a transfer process is described as a simple rate constant, k, with units of reciprocal time (min^{-1}). The rate constant can be related to the half-time of the process ($t_{1/2}$, with units of min):

$$t_{1/2} = \frac{ln2}{k} \qquad (2)$$

The physiological tissue attributes of blood flow (F), permeability (P) and capillary surface area (A or S) were first incorporated into an expression for unidirectional flux across a single capillary by Renkin (1959) and Crone (1963):

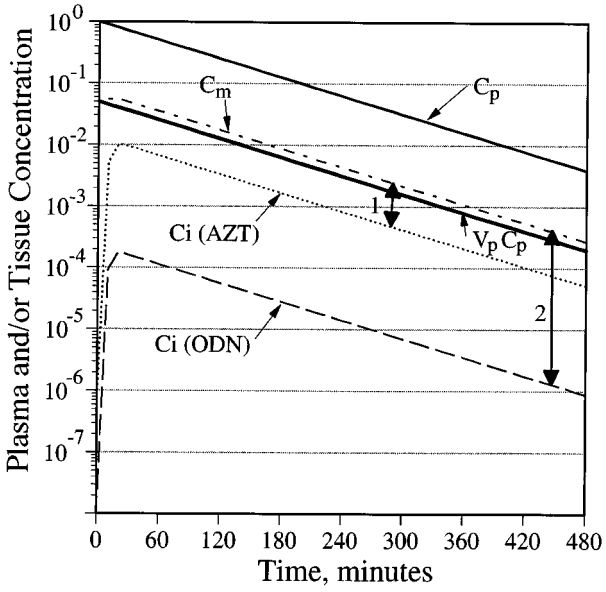

Figure 3 Time course of drug concentration. The concentration time course of two drugs with a plasma half-life of 60 min, no protein binding, and no metabolism has been modeled with a two compartment model. C_p represents plasma concentration of free drug. C_m is the concentration of drug that would be measured in a sample of brain, which at any point in time would consist of two components: Ci (the amount in brain extra and intracellular fluid), and V_pC_p, which represents the amount of drug in the vascular space compartment of brain. The time course of brain concentration has been modeled for AZT {Ci (AZT)} using the influx and efflux constants of Galinsky *et al*, (1990) and Equation 7. The time course for tissue concentration of a drug with an influx constant near that of oligonucleotides {Ci (ODN)} is also shown, for which $K_1=10^{-5}$ ml/g/min. Arrow 1 indicates the overestimation with a drug that has properties like AZT and arrow 2 indicates the overestimate for the ODN.

$$E = 1 - e^{-PS/F} \quad (3)$$

where E is the extraction fraction (the fraction of solute removed during one capillary passage). In practice, experiments to directly measure E are difficult to perform in the brain because of both timing and sampling issues. In 1978, Rapoport and colleagues (Ohno *et al*, 1978) developed a method to measure the permeability-surface area product (referred to as both PS and PA in the literature) of water-soluble solutes and in 1983 Blasberg *et al* published a similar method that expressed transcapillary transfer as a clearance constant, K (Blasberg *et al*, 1983b). These terms can be interrelated:

$$K = EF \quad (4)$$

$$K = F\ (1 - e^{-PS/F}) \quad (5)$$

where F is blood or plasma flow. These interrelationships increase the usefulness of E, PS, and K as expressions of transcapillary transfer in the brain since and facilitate understanding of experiments conducted with different methods in different laboratories. Both PS and K, which can be determined from carefully selected single-time point (Blasberg *et al*, 1983a) or multiple-time point experiments (Ohno *et al*, 1978; Patlak *et al*, 1983; Blasberg *et al*, 1983b), are now a common means of expressing the rate of blood-to-brain movement of passively-distributed solutes. Occasionally BBB results are expressed in terms of a permeability coefficient, P, with units of velocity (cm/min). In these instances the experiments are often conducted to measure a PS or K and the result divided by a value of S (brain capillary surface area, cm^2/g) obtained from the literature, since neither P nor S can be directly measured by *in vivo* experiments in brain.

These terms are also useful for expressing drug delivery to brain tissue. The amount of drug *available* for exchange across brain capillaries (A) is dependent on the plasma concentration of free drug (C_p), blood flow (F), and the fraction of blood volume that serves as the source for the solute (V_f):

$$A_0^T = FV_f \int_0^T C_p(t)dt \quad (6)$$

The integrated time course of free drug concentration in blood or plasma ($\int_0^T C_p(t)dt$), often referred to as the concentration times time product (C × T product) or the 'Area Under the Curve' (AUC), provides the force that drives blood-to-brain transfer. In the simplest situation, in a two compartment model (brain and blood) in which a drug crosses the BBB by diffusion and there is no plasma binding and no diffusion in brain tissue, the concentration of drug in brain tissue (Blasberg and Groothius, 1986) can be described by:

$$Ci(T) = K_1 \int_0^T C_p(t)e^{-(k_2+k_3)(T-t)}dt \quad (7)$$

where K_1 (equivalent to K in Equations 2 and 3) has units of ml/g/min and k_2 (brain efflux constant) and k_3 (tissue metabolism constant) have units of reciprocal time (min^{-1}). Equation 7 can be used to calculate tissue drug concentration over time.

In order to accurately measure the transfer process between different compartments in the brain, the method used to measure the brain concentration (Ci) must be accurate. Recently, microdialysis has become a popular analytic tool to measure ECF concentrations in different tissues (Stahle, 1993), including brain (Boschi *et al*, 1995; de Lange *et al*, 1995; Parsons and Justice, 1994). This method of sampling avoids the issues of contamination by drug within the vascular space. However, the process of inserting a probe may injure the BBB and result in increased drug concentrations around the probe. A common process for microdialysis in brain involves initial insertion of a guide cannula, followed at a later time (usually 1–7 days after insertion of the guide cannula and 1–2 h before an experiment) by insertion of a microdialysis probe, which extends approximately 1–3 mm below the tip of the guide cannula. The BBB can be disrupted around the cannula and the probe (Morgan *et al*, 1996; Westergren *et al*, 1995), although the time course of the disruption has not yet been established. Morgan *et al* (1996) compared the measurement of BBB transport of sucrose and urea using a 'classic' method and microdialysis: the influx constant of sucrose was 0.026×10^{-2} min^{-1} with the 'classic' method and 1.3×10^{-2} min^{-1} with microdialysis, a 50-fold difference. The magnitude of the measurement error was less for urea than sucrose, suggesting that the more restricted the passage of a compound across the normal BBB, the larger the magnitude of measurement error with microdialysis.

In summary, the BBB may be viewed as a continuous tubular membrane across which most therapeutic antiviral and antiretroviral drugs must pass by infusion. Several different methods have been developed to measure, and to express, the blood–brain exchange process. However, care must be taken to assure that the experimental methods account for drug remaining within the vascular space (V_pC_p) at the termination of an experiment, as well as assuring that measurements of brain drug concentration (Ci) are not perturbed by the experimental methodology.

The blood–CSF barrier Like the BBB, the production and movement of CSF (blood⇄CSF) has been well characterized (Davson and Segal, 1996; Fishman, 1980; Wood, 1980). CSF is largely produced in the choroid plexuses of the cerebral ventricles. The choroid plexus, an organ that protrudes into the ventricles, contains continuous, fenestrated capillaries (Figure 2b). Fenestrations, which are found in other organs in the body, allow small molecular weight compounds to cross, but increasingly restrict the movement of large molecules, a process called permselectivity (Rapoport, 1983). Once a solute has crossed the capillary wall, it must also cross the choroidal epithelium before entering the CSF. The choroidal epithelium also regulates the composition of the CSF, often involving active transport processes. The apices of the choroidal epithelium are joined by tight junctions, but these do not form a continuous barrier like that of the BBB and allow some bulk fluid to occur (Rapoport, 1983). Once in the CSF, solutes are carried by bulk flow as the CSF moves through the lateral ventricles into the IIIrd and IVth ventricles and then out through the foramina of Luschka and Magendie into the spinal subarachnoid space, which has been referred to as the 'third circulation' (Milhorat, 1975). CSF production varies between 2 μl/min in the rat to 350 μl/min in man. In the subarachnoid space, CSF continues to move by bulk flow over the convexities of the cerebral hemispheres before emptying into the saggital sinus via the arachnoid granulations. Once CSF enters the subarachnoid space, which contains about 80% of the total CSF, flow patterns and velocities become more complex. Magnetic resonance imaging techniques have shown that the CSF has a pulsatile movement, driven by the expansion and relaxation of intracerebral blood vessels during the cardiac cycle, and that the velocity of CSF movement varies considerably at different points throughout the ventricular system and subarachnoid space (Bradley, 1992; Greitz, 1993). Unlike the sampling problems associated with studies of the BBB, CSF can be directly sampled, which is easily done with multiple-time point samples in both animals and man (Nau *et al*, 1993). However, even in steady state conditions there is marked regional variation in CSF protein concentration, indicating that the system is not well mixed and has regional variation in bulk flow pathways.

In summary, CSF is initially produced across choroid plexus capillaries by a process resembling ultrafiltration. This fluid must also cross the choroidal epithelium, where active transport processes intervene to regulate the CSF composition of many compounds, including nucleosides. Once formed, the CSF moves by bulk flow through the ventricular system and into the subarachnoid space, where it flows around the surface of the brain and exits into the venous system.

Exchange between CSF and ECF In contrast to blood⇄ECF and blood⇄CSF exchange, exchange between CSF and ECF is more complicated. While in the ventricular system, CSF can exchange with ECF across the ependymal lining (Figure 2c), which varies in structure along its course. Ependymal cells are joined by tight junctions in some areas, where the most common pathway for solute entry is by diffusion, but discontinuous gap junctions can be found in other areas, where bulk flow is possible. In the ventricular system, either gray or white matter may lie under the ependyma. Once in the subarachnoid space, the CSF moves over the surface of the brain through the loosely organized cells of the pia mater and over the glia limitans, which is comprised of astrocytic processes that cover the brain surface (Figure 2d). Although the glia limitans is covered by a basement membrane, there is no intercellular junctional apparatus. In the ventricular system 50% of the ventricular surface overlies white matter (Rosenberg *et al*, 1980), while in the subarachnoid space the CSF overlies the gray matter of the cerebral and cerebellar cortex. Recently, Ghersi-Egea *et al* demonstrated regional variation of ^{14}C-sucrose diffusion into brain at CSF-brain interfaces, along with ultrastructural differences in the glia limitans, suggesting that the concept of a restrictive 'CSF-brain barrier' may be true in some locations (Ghersi-Egea *et al*, 1996).

The structure of the CSF⇄ECF interface will permit bulk flow to occur in either direction (CSF→ECF or ECF→CSF), depending upon the local osmotic and hydrostatic pressure gradients, and will allow diffusion to occur if the pressure gradients are balanced and bulk flow is absent. Cserr *et al* developed a model of CSF⇄ECF exchange in which the flow of brain ECF and of CSF was envisioned to occur in parallel, with variable interchange across the CSF–ECF interface (Figure 4) (Cserr *et al*, 1977). This model allows for bidirectional exchange across the pia-ependyma by either diffusion or bulk flow, but emphasizes that the movement of CSF and ECF normally occurs as parallel processes, where net efflux (k_{out}) can be represented by:

$$k_{out} = k_{BBB} + k_{CSF} + k_x \qquad (8)$$

where k_{BBB} represents efflux across the BBB, k_{CSF} represents efflux into CSF, and k_x represents efflux by undefined pathways (Cserr *et al*, 1981). The normal direction and magnitude of CSF bulk flow and diffusion have been partially characterized in the laboratory. In the cat, Rosenberg *et al* established that the normal direction and velocity of the bulk flow component in white matter is from ECF→CSF, with a velocity of 10.5 μm/min and a volume of 7.4 μl/min and estimated that this pathway accounted for 33% of normal CSF production (Rosenberg *et al*, 1980). There was no bulk flow

component in gray matter. Cserr *et al* found that compounds varying in molecular weight from 900–69 000 daltons were removed from the rat brain at the same rate regardless of size, with an efflux constant of k_{out}=0.045–0.057 h^{-1} and a maximum rate of ECF removal of 0.11 $\mu l\ g^{-1}\ min^{-1}$ (Cserr *et al*, 1981). Using a different experimental system, Rapoport *et al* also demonstrated efflux of ^{14}C-urea into CSF, as well as across capillary walls (Rapoport *et al*, 1982).

Solute movement in the opposite direction (CSF→ECF) has been studied by the technique of ventriculo-cisternal (VC) perfusion, in which CSF concentrations were maintained at constant levels. These studies have shown that solute entry from CSF into brain ECF normally occurs by diffusion (Fenstermacher *et al*, 1970; Blasberg *et al*, 1975, 1977; Patlak and Fenstermacher, 1975; Blasberg, 1977; Kessler *et al*, 1976). Drug movement from CSF to brain ECF is very inefficient for reaching large volumes of brain. In accordance with a diffusion driven process, drug concentration decreases exponentially from the brain surface and the penetration distance is generally measured in millimeters at steady-state conditions. In contrast to a typical distance between CSF interfaces in the rat brain of 3–4 mm, Blasberg estimated the distance in the human brain to be 1–1.5 cm, with a maximal distance of 3.5 cm through the basal ganglia (Blasberg *et al*, 1977). In this context, he presented an analysis of time–distance–concentration profiles for methotrexate in brain after intraventricular administration, and concluded that 'diffusional transport to periventricular or peri-pia-glia tissue is rapid, but is a very slow means of transport to deep brain tissue' (Blasberg *et al*, 1977). For example, at a 5 mm distance from CSF interfaces, the concentration of the nucleoside analog cytosine arabinoside was about 0.0005 times the CSF concentration after a 4 h VC perfusion (Blasberg, 1977). Figure 5 illustrates a 5 mm distance from the brain surface in a coronal section of human brain and indicates the deeper brain regions that will escape significant exposure from drugs in the CSF. Recognizing the importance of the diffusion gradient, Collins and Dedrick proposed a 'distributed model' of CSF⇄ECF exchange, which emphasized that the concentration of a drug in brain tissue was dependent upon *both* the location *and* the time at which the sample was taken ($C_{x,t}$), as well as the properties of the solute, and that since the bulk flow removal of CSF is orders of magnitude higher than rates of diffusion, water-soluble drug entry deep into underlying brain was minimal (Collins and Dedrick, 1983).

In summary, solute exchange between the CSF and ECF is highly variable with regard to: (1) time, (2) the distance between the CSF interface and the brain in which measurements are made, and (3) the type of brain involved (gray *vs* white matter). There

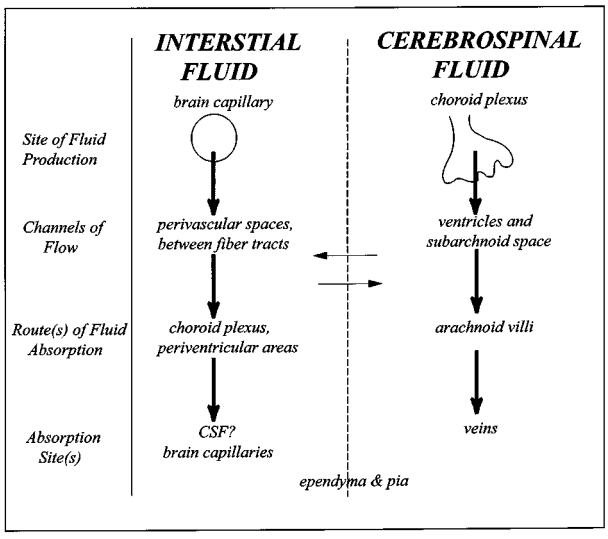

Figure 4 Diagrammatic representation of the CSF–ECF fluid pathways (after Cserr *et al* 1977). This model of bulk fluid flow in brain interstitial fluid and cerebrospinal fluid emphasizes that these two processes occur in parallel and largely independent. Exchange between the two compartments can occur *in either direction*, depending upon the local hydrostatic and osmotic pressure environments, and if these forces are balanced between the two compartments, by diffusion along a concentration gradient.

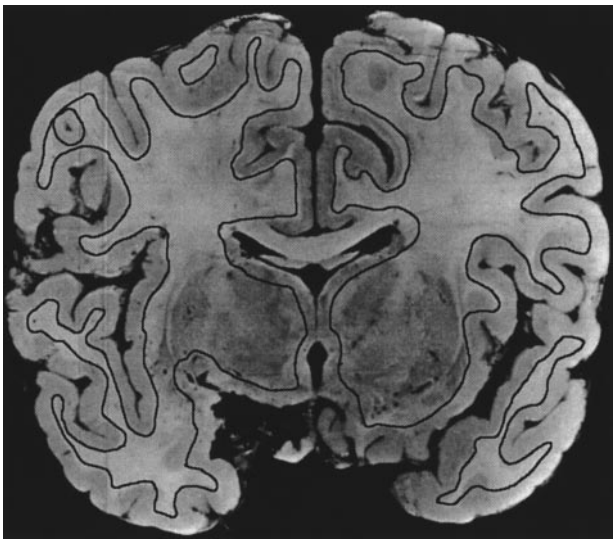

Figure 5 Brain penetration of drug from CSF. A coronal section of human brain is shown, at the level of the thalamus and basal ganglia. The black line is drawn approximately 5 mm from any brain surface in contact with CSF. After a 4 h ventriculo-cisternal perfusion brain concentrations of cytosine arabinoside will have fallen to approximately 0.0005 times their concentration in CSF at the brain depth indicated by the line. Extensive areas of brain, including both gray and white matter, will escape significant exposure to the drug.

is normally a bulk flow component from ECF→CSF that will impede the entry of drugs from the CSF into the ECF. Instead, this bulk flow process removes drug from brain ECF. Over gray matter, exchange appears to be predominantly diffusional and the direction will depend upon which compartment has the higher concentration. However, even if CSF concentrations exceed ECF concentrations and diffusion does occur into brain, drug penetration of more than a few millimeters is minimal. A direct and important consequence of the complexity of CSF⇄ECF exchange is that ECF concentrations cannot easily be extrapolated from CSF concentrations, and that at distances over a few mm from the brain surface any relationship between CSF concentration and ECF concentration is largely abrogated.

Summary: physiological and pharmacokinetic model Figure 6 illustrates a physiological model of brain that includes the four major compartments described in this review: blood, CSF, and brain extracellular and intracellular spaces. This model is based on the previous discussion as well as work by other investigatiors (Cserr *et al*, 1977; Blasberg, 1977; Rapoport *et al*, 1982; Blasberg *et al*, 1983b; Collins and Dedrick, 1983; Patlak *et al*, 1983; Blasberg and Groothuis, 1986; Robinson and Rapoport, 1990; Walker and Cook, 1996). The model indicates barrier systems between CSF and brain ECF, the nature of which will depend upon the specific location of the interface, e.g. ependyma *vs* glia limitans, and allows for movement between adjacent brain regions, which may occur by either bulk flow or diffusion. The rate of change of drug concentration in the brain extracellular compartment can be described in a lumped model by the following differential equation:

$$\frac{dC_{ecf}}{dt} = K_1 C_p + k_4 C_{icf} + k_6 C_{CSF} - (k_2 + k_3 + k_5) C_{ecf} \qquad (9)$$

Where K_1 is the blood-to-brain transfer constant, k_2 is the brain-to-blood efflux constant, k_3 and k_4 are influx and efflux constants across brain cell membranes, and k_5 and k_6 are CSF:brain influx and efflux constants.

Antiviral and antiretroviral drug entry into the brain

Antiviral drugs, especially antiretroviral drugs used to treat HIV infection, presently fall into four classes: nucleoside analogs, protease inhibitors, non-nucleoside reverse transcriptase inhibitors, and antisense oligonucleotides.

Antiviral nucleosides A recent review of antiretroviral nucleoside entry into the nervous system concluded that anti-HIV nucleosides penetrate the BBB poorly and drug delivery is less than optimal (Gallo, 1994). Using the model of CSF⇄ECF

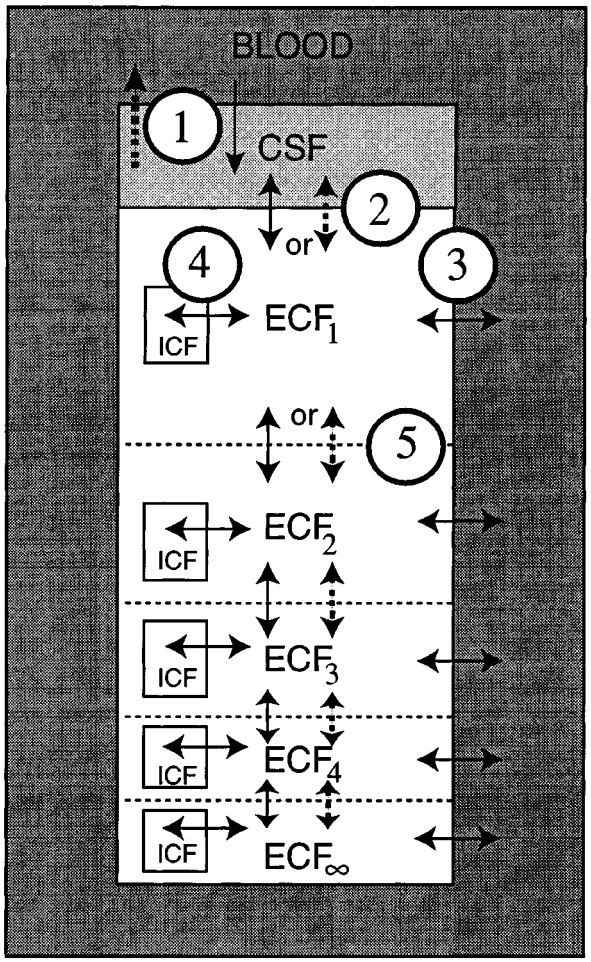

Figure 6 Physiological model of brain for antiviral drugs. Four major compartments are shown: blood, cerebrospinal fluid (CSF), brain extracellular fluid (ECF), and brain intracellular fluid (ICF). Solid arrows indicate movement between compartments by simple diffusion. Dotted arrows indicate movement by bulk flow. The arrowheads indicate the direction of solute movement. The ECF 'compartments' are numbered 1–4, and ∞, to indicate that ECF is not necessarily homogeneous and that some compartments may be large distances from the CSF. The principle exchange processes are indicated by numbers in circles: (1) Between blood and CSF, solute movement is largely by ultrafiltration into CSF, and a simple bulk flow process removes CSF into the saggital sinus. (2) Between CSF and ECF, fluid and solute exchange may occur either in either direction by bulk flow or diffusion, depending upon the location (e.g. ventricle *vs* subarachnoid space) and the type of brain involved (gray *vs* white matter). (3) Exchange between blood and ECF is by simple diffusion for most antiviral drugs, except in specialized areas. (4) Exchange between ECF and ICF will occur by simple diffusion for most antiviral drugs. (5) Fluid and solute exchange between different ECF regions may be either diffusional or by bulk flow. Current evidence suggests that exchange is predominantly diffusional in gray matter and by bulk flow in white matter. In many disease states, e.g. brain tumors, a new bulk flow component is added and dominates exchange between adjacent brain compartments.

exchange presented above (Figure 6, Equation 9), it is helpful to reexamine published studies concerning antiretroviral drug entry into the brain. A recurring theme in the clinical literature is that brain ECF concentrations can be related to CSF concentrations. This concept is inaccurate: CSF concentrations cannot reliably be used as estimates of ECF concentrations, except perhaps very near the brain surfaces. In addition, the methodology of each study must be carefully evaluated before accepting or rejecting its conclusions. Studies that express results in terms of uncorrected brain:plasma ratios may overestimate the amount of drug in the brain. Studies that employ microdialysis, which can damage the BBB, may overestimate brain ECF concentrations of antiretroviral nucleosides unless precautions were taken to assure that BBB function had returned to normal.

Azidothymidine (3′-Azido-3′-deoxythmidine, AZT, zidovudine) Of the published studies about AZT entry into brain, there are two (Galinsky *et al*, 1990; Terasaki and Pardridge 1988) that did not express results as brain:plasma ratios and that did not use microdialysis. Terasaki *et al* measured the brain uptake index (BUI) of AZT, DDC (2′-3′-dideoxycytidine), and DDA (2′-3′-dideoxyadenosine) using ^{14}C-butanol and ^{14}C-sucrose as the blood flow-limited and permeability-limited references, respectively, and found BUI values of $<2\%$ for each nucleoside analog, a value similar to that of sucrose. Terasaki and Pardridge concluded that neither AZT nor the nucleosides DDC or DDA were measurably transported through the BBB and that the transfer rate was slow. Galinsky *et al*, in addition to reporting the concentration of AZT in plasma, CSF, and brain of rats, both corrected and uncorrected for vascular space, used compartmental analysis to calculate K_1 (0.59 μl/g/min) and k_2 (0.044 min^{-1}) (Galinsky *et al*, 1990). The extent to which this influx constant represents the limited BBB permeability of AZT can also be illustrated by using Equation 4 to calculate the extraction fraction (i.e. the fraction of blood passing through the brain from which AZT is removed). If blood flow (F) is 1 ml/g/min, and AZT is not protein bound, then $E=K_1/FV_f$, where $V_f \sim 0.6$ (plasma fraction), or, E=0.00098. In other words, less than 0.1% of AZT passing through brain capillaries is removed by the brain.

These measurements of brain transcapillary transfer for AZT can be used to calculate the time course of AZT in brain, which can then be compared to AZT concentrations known to inhibit HIV replication. Based on information from systemic administration of 200 mg oral or 2.5 mg/kg intravenous doses of AZT, peak plasma concentrations of about 1 mg/L (=1 μg/ml) may be expected (Burger *et al*, 1995; Dudley, 1995). The time-activity course of AZT in plasma and brain ECF may be calculated from Equation 7, where Ci(T) is the concentration of AZT in brain, and k_3 is a metabolism constant. During an 8 h period after administration, a maximum brain ECF concentration of 0.01 μg/ml would be expected if it assumed that $k_3=0$ (Figure 3). This expected brain concentration of AZT after a single dose can be compared to AZT concentrations reported to inhibit HIV-1 replication. Sensitive strains of HIV-1 respond to <0.2 μM AZT (=0.054 μg/ml), while resistant strains may not respond to >1 μM AZT (=0.27 μg/ml) (Kimberlin *et al*, 1995). Thus, the peak level of AZT in brain with this administration schedule would be expected to be five times less than the lowest concentration needed to effectively inhibit HIV-1 replication. It is important to note that this modeling assumes the *best* possible case for AZT entry into the brain. It does not take into account bioavailability after oral administration, plasma protein binding, tissue metabolism in pathways other than phosphorylation, or other efflux pathways from the brain, all of which would act to reduce brain tissue concentrations of AZT and its active, phosphorylated metabolites.

Other antiviral nucleoside analogs All but one of the published studies of BBB transfer of other antiviral nucleoside analogs have used CSF:plasma, brain:plasma ratios, or simple measures of brain concentrations to express the extent of brain uptake. This includes studies of Acyclovir [9-(2-hydroxyethoxymethyl) guanine], Cytarabine (Ara-C; cytosine arabinoside), Didanosine (ddI; 2′,3′-dideoxyinosine), Ganciclovir (9-[[2-hydroxy-1-(hydroxymethyl)ethoxy]methyl]guanine), Lamivudine (3TC; 2′-deoxy-3′-thiacytidine), Stavudine (d4T; 2′,3′-didehydro-3′-deoxythymidine), Vidarabine (Ara-A, adenine arabinoside) and Zalcitabine (ddC). The exception was a study of the uptake kinetics of ddI by Anderson *et al*, who used multiple time point experiments and nonlinear curve fitting to estimate K_1 (0.35 μl/g/min) and k_2 (0.051 min^{-1}), respectively (Anderson *et al*, 1990). These values are close to that for AZT (Galinsky *et al*, 1990), and emphasize the extent to which the BBB is likely to impede the brain entry of the nucleoside analogs.

Protease inhibitors Unlike the nucleoside analogs, the protease inhibitors represent a chemically heterogeneous group of drugs (Table 2), of which three are currently approved for clinical use. There is little published information about the ability of the protease inhibitors to cross the BBB, and little published information about their physicochemical properties (e.g. octanol:water solubility) that permits speculation about the rate of BBB transfer. Some protease inhibitors, including saquinavir, have octanol:water partition coefficient values indicating high lipid solubility (West and Fairlie, 1995), which favors entry across the BBB. Lin *et al*

Table 2 Physicochemical properties of protease inhibitors and non-nucleoside reverse transcriptase inhibitors

	Protease Inhibitors			*NNRTIs*	
	Ritonavir (Norvir)	*Indinavir (Crixivan)*	*Saquinavir (Invirase)*	*Nevirapine (Viramune)*	*Delavirdine*
Molecular weight	720.95	711.88	766.96	266.3	552.68
$t_{1/2}\beta$ (hr)	3–5	2	7–12	31	3–7[a]
%Protein binding	>98	60	>98	55	NA
Log $P_{o/w}$	NA	NA	4.1	1.8	NA
K_1 (ml/g/min)	NA	0.19	NA	NA	NA

The plasma elimination half-times and percent protein binding values represent data from a variety of sources in the literature. The log $P_{o/w}$ for saquinavir is from West and Fairlie (1995), and the K_1 of Indinavir was calculated from the data of Lin *et al* (1996), as decribed in the text. The superscript a for delavirdine indicates that the plasma pharmacokinetics are nonlinear. NA indicates that information is not available.

studied the brain entry of indinavir in rats and measured a BUI and steady state brain:plasma ratios (corrected for vascular space) (Lin *et al*, 1996). The BUI was determined to be 0.33 and E was estimated to be 0.19. Although the authors concluded that BBB penetration was limited, these results suggest that indinavir crosses the BBB more rapidly than the nucleoside analogs. From Equation 2, when F=1 ml/g/min, K_1 can be calculated to be 0.19 ml/g/min, which is 300 times greater than the K_1 of AZT. Denissen *et al* measured tissue:plasma ratios of ritonavir (not corrected for tissue plasma space) and concluded that ritonavir does not appreciably cross the BBB in rats (Denissen *et al*, 1997). The brain entry of this group of drugs needs to be studied in more detail.

Non-nucleoside reverse transcriptase inhibitors (NNRTIs) Like the protease inhibitors, the NNRTIs represent a chemically diverse group, of which nevirapine is clinically available and delavirdine is in clinical trials (Table 2). Also like the proteas inhibitors, very little information about BBB entry is available. The ability of nevirapine to cross an *in vitro* model of the BBB was reported as fivefold higher than AZT and tenfold higher than nevirapine, while the penetration of delavirdine was below the level of detection by the assay (Yasdanian, 1997). In recent abstracts, nevirapine plasma:brain ratios (not corrected for tissue plasma space) were reported as 1 : 1.1 in the monkey and 1 : 0.99 in the rate (Silverstein, 1996). Published studies describing these experiments are not yet available.

Antisense oligonucleotides In contrast to the controversy about the brain uptake of nucleoside analogs, most investigators acknowledge that antisense oligonucleotides (ODNs) cross the BBB poorly. Boado has reviewed many issues associated with ODNs and the BBB (Boado, 1995). Antisense oligonucleotides are large, highly water-soluble compounds: a 20 mer phosphorothioate ODN has a molecular weight of about 6 kD and a log P octanol:water solubility of approximately −5.48 (K Schlageter, Ph.D., unpublished communication), compared to log P values of −1.5–3 for the nucleosides and their analogs, and log P values greater than two for some of the protease inhibitors. Most of the published studies of ODN uptake into brain have emphasized the significance of BBB limitations and have expressed results either as a percentage of injected dose or units (μg or c.p.m.) per unit weight of tissue (Agrawal *et al*, 1991; Chem *et al*, 1990; Cossum *et al*, 1993; Saijo *et al*, 1994; Iversen *et al*, 1995; Crooke *et al*, 1996). Kang *et al* found a K_1 value for a 36-mer 3′-biotinylated phosphodiester ODN of 0.57 μl/g/min, which is surprisingly high (Kang *et al*, 1995). The authors state, however, that brain uptake of free ^{32}P label may account for the artificially or erroneously high value. Wu *et al* (1996) found the K_1 of an 18-mer phosphorothioate ^{3}H-labeled ODN to be 0.049 μl/g/min and estimated that 0.018% of the injected dose per gram was delivered to brain. Boado *et al* found K_1=0.1 μl/g/min for an ^{125}I-labeled phosphorothioate ODN with a single internal phosphodiester bond. Antisense oligonucleotide delivery to brain needs to be studied in more detail, and the relationships determined between the rate of brain entry and nucleotide sequence, the chemical structure of the backbone, and oligonucleotide sequence length.

Alternative methods for delivering antiviral and antiretroviral drugs to brain

A primary focus of this review has been to emphasize that drug exchange between blood, cerebrospinal fluid, and brain extracellular fluid does not occur freely, and that drug concentration measurements made in any one of these compartments may not accurately reflect events in the other compartments. It appears that antiviral and antiretroviral drugs, with the possible exception of one or more of the protease inhibitors, will not reach therapeutic concentrations in the brain after oral, intravenous, or even intraventricular administration. Delivery of antiviral and antiretroviral drugs to the brain remains a significant treatment issue, particularly since undertreatment of brain infection in the face of effective systemic treat-

ment may create a viral sanctuary, from which the brain could reseed the body and allow the disease to recur.

Many alternative methods are being explored to increase antiviral drug therapy to brain. For example, many different approaches are being used to increase brain concentrations of AZT. If brain efflux of AZT is mediated by an active or facilitated pathway, as suggested by some studies, then inhibiting that system will prolong the residence time of AZT in brain extracellular fluid. Probenecid, which inhibits weak acid transport in the kidney and CSF, may inhibit the efflux of AZT from brain (Dykstra *et al*, 1993; Wong *et al*, 1993). Since these studies employed microdialysis, their significance is as yet unclear. A study across an *in vitro* capillary system was unable to demonstrate any effect of probenecid (Masereeuw *et al*, 1994), although a more recent *in vitro* study supports an effect of probenecid (Takasawa *et al*, 1997). Many different groups have tried to increase brain uptake of AZT by using chemical delivery systems (Brewster *et al*, 1993), chemically modifying AZT to increase its lipid solubility (Chu *et al*, 1990), or creating prodrug forms of AZT (Wang *et al*, 1996).

Prodrugs (Greenwald, 1997), colloidal nanoparticles (Davis, 1997), and virally-mediated gene delivery (Fink *et al*, 1996) represent promising new delivery techniques. Pardridge and colleagues (Kang *et al*, 1995; Wu *et al*, 1996) have explored the possibility of using vector-mediated systems and peptide nucleic acids as carriers for ODNs, which have increased the amount of ODN reaching brain ECF. Others have explored injections of ODNs into CSF (Whitesell *et al*, 1993; Yaida and Nowak, 1995) or directly into brain (Szklarczyk and Kaczmarek, 1995; Yaida and Nowak, 1995). For reasons we have discussed, CSF administration is likely to result in inadequate tissue penetration, and will be associated with rapid removal of ODNs by bulk flow of CSF. Short term, direct intracerebral administration of ODNs has been used to effectively block CNS function without significant neurotoxicity (McCarthy *et al*, 1993, 1995; Sakai *et al*, 1994, 1995; Lu *et al*, 1995), demonstrating that ODNs can be effective once after entering the brain extracellular space. However, neurotoxicity remains a critical issue; repeated administration of a phosphorothioate. DN was associated with neurotoxicity (Chlasson *et al*., 1996) and phosphorothioate ODNs have been reported neurotoxic at concentrations greater than 1 μM (Agrawal, 1991). Newer direct delivery methods, such as convection-enhanced delivery from microinfusions into brain tissue (Bobo *et al*, 1994; Morrison *et al*, 1994) have not yet been used clinically with antiviral and antiretroviral drugs, although our preliminary experience has been encouraging (Levy *et al*, 1997). As these new methods of drug delivery to the CNS are being explored, we are confident that careful pharmacokinetic studies of drug delivery, combined with studies of drug metabolism within the CNS and studies of neurotoxicity, can identify effective means to deliver therapies for viral brain diseases, including AIDS.

References

Agrawal S (1991). Prospects for Antisense Nucleic Acid Therapy of Cancer and AIDS. In *Prospects for Antisense Nucleic Acid Therapy of Cancer and AIDS*. Wickstrom E (ed): Wiley-Liss: New York, pp. 142–158.

Agrawal S, Temsamani J *et al* (1991). Pharmacokinetics, biodistribution, and stability of oligodeoxynucleotide phosphorothioates in mice. *Proc Natl Acad Sci USA* **88:** 7595–7599.

Anderson BD, Hoesterey BL *et al* (1990). Uptake kinetics of 2′,3′-dideoxyinosine into brain and cerebrospinal fluid of rats; intravenous infusion studies. *J Pharmacol Exp Ther* **253:** 113–118.

Archer DP, Labrecque P *et al* (1987). Cerebral blood volume is increased in dogs during administration of nitrous oxide or isoflurance. *Anesthesiology* **67:** 642–648.

Artru AA (1987). Reduction of cerebrospinal pressure by hypocapnia: changes in cerebral blood volume, cerebrospinal fluid volume, and brain tissue water and electrolytes. *J Cereb Blood Flow Metab* **7:** 471–479.

Betz AL, Goldstein GW *et al* (1994). Blood–Brain–Cerebrospinal Fluid Barriers. In *Basic Neurochemistry: Molecular, Cellular and Medical Aspects*. Siegel GJ (ed): Raven Press: New York, pp. 681–699.

Blasberg RG (1977). Methotrexate, cytosine arabinoside, and BCNU concentration in brain after ventriculocisternal perfusion. *Cancer Treat Rep* **61:** 625–631.

Blasberg RG, Groothuis DR (1986). Chemotherapy of brain tumors: physiological and pharmacokinetic considerations. *Sem Oncol* **13:** 70–83.

Blasberg RG, Patlak C *et al* (1975). Intrathecal chemotherapy: brain tissue profiles after ventriculocisternal perfusion. *J Pharmacol Exp Ther* **195:** 78–83.

Blasberg RG, Patlak CS *et al* (1977). Distribution of methotrexate in the cerebrospinal fluid and brain after intraventricular administration. *Cancer Treat Rep* **61:** 633–641.

Blasberg RG, Patlak CS *et al* (1983a). Selection of experimental conditions for the accurate determination of blood–brain transfer constants from single-time experiments: a theoretical analysis. *J Cereb Blood Flow Metab* **3:** 215–225.

Blasberg RG, Patlak CS *et al* (1983b). The transport of alpha-aminoisobutyric acid across brain capillary and cellular membranes. *J Cereb Blood Flow Metab* **3:** 8–32.

Boado RJ (1995). Antisense drug delivery through the blood–brain barrier. *Advanced Drug Deliv Rev* **15:** 73–107.

Boado RJ, Kang Y-S, *et al*. (1995). Rapid plasma clearance and metabolism *in vivo* of a phosphorothioate oligodeoxynucleotide with a single, internal phosphodiester bond. *Drug Metab Disp,* **23,** 1297–1300.

Bobo RH, Laske DW *et al* (1994). Convection enhanced delivery of macromolecules in the brain. *Proc Natl Acad Sci USA* **91:** 2076–2080.

Boschi G, Launay N *et al* (1995). Brain microdialysis in the mouse. *J Pharmacol Toxicol Meth* **33:** 29–33.

Bradbury M (1979). *The Concept of a Blood-Brain Barrier*. J. Wiley: New York.

Bradbury MWB (1992). *Physiology and Pharmacology of the Blood–Brain Barrier*. Springer Verlag: Berlin.

Bradley WG (1992). Magnetic resonance imaging in the evaluation of cerebrospinal fluid flow abnormalities. *Magn Reson Quart* **8:** 169–196.

Brewster ME, Pop E *et al* (1993). The effect of dihydronicontinate N-substitution on the brain targeting efficacy of a zidovudine chemical delivery system. *Pharm Res* **10:** 1356–1362.

Budinger TF, Huesman RH (1985). Ten precepts for quantitative data acquisition and analysis. *Circulation* **72** (Suppl 4): 53–62.

Burger DM Meenhorst PL *et al* (1995). Concise overview of the clinical pharmacokinetics of dideoxynucleoside antiretroviral agents. *Pharm World Sci* **17:** 25–30.

Chem T-L, Miller PS *et al* (1990). Disposition and metabolism of oligodeoxynucleoside methylphosphonate following a single iv injection into mice. *Drug Metab Disp* **18:** 815–818.

Chlasson BJ, Hong M *et al* (1996). Antisense therapeutics in the central nervous system: the induction of c-fos. In *Antisense Therapeutics*. Agrawal S (ed): Humana Press: Totowa, N.J., pp. 225–246.

Chu CK, Bhadti VS *et al* (1990). Brain targeting of anti-HIV nucleosides: synthesis and *in vitro* and *in vivo* studies of hihydropyridine derivatives of 3′-azido-2′,2′-dideoxyuridine and 3′-azido-3′-dideoxythymidine. *J Med Chem* **33:** 2188–2192.

Cohn SE, Nawaz T *et al* (1996). Antiviral Agents. In *A Practical Approach to Infectious Diseases*. Reese RE, Betts RF (ed): Little, Brown and Co.: Boston, pp. 967–1036.

Collins JM, Dedrick RL (1983). Distributed model for drug delivery to CSF and brain tissue. *Am J Physiol* **14:** R303–R310.

Cornford EM, Oldendorf WH (1975). Independent blood-brain barrier transport systems for nucleic acid precursors. *Biochim Biophys Acta* **394:** 211–219.

Cossum PA, Sasmor H *et al* (1993). Disposition of the ^{14}C-labeled phosphorothioate oligonucleotide ISIS 2105 after intravenous administration to rats. *J Pharmacol Exp Ther* **267:** 1181–1190.

Cremer JE, Seville MP (1983). Regional brain blood flow, blood volume and hematocrit values in the adult rat. *J Cereb Blood Flow Metab* **3:** 254–256.

Crone C (1963). The permeability of capillaries in various organs as determined by the use of the 'indicator diffusion' method. *Acta Physiol Scand* **59:** 292–305.

Crooke ST, Graham MJ *et al* (1996). Pharmacokinetic properties of several novel oligonucleotide analogs in mice. *J Pharmacol Exp Ther* **277:** 923–937.

Cserr HF, Cooper DN *et al* (1977). Flow of cerebral interstitial fluid as indicated by the removal of extracellular markers from rat caudate nucleus. *Exp Eye Res* **25** (Suppl): 461–473.

Cserr HF, Cooper DN *et al* (1981). Efflux of radiolabeled polyethylene glycols and albumin from rat brain. *Am J Physiol* **240:** F319–F328.

Davis SS (1997). Biomedical applications of nanotechnology–implications for drug targeting and gene therapy. *TIBTECH* **15:** 217–224.

Davson H, Segal MB (1996). Physiology of the CSF and Blood–Brain Barriers. CRC Press: Boca Raton.

de Lange EC, Hesselink MB *et al* (1995). The use of intracerebral microdialysis to determine changes in blood–brain barrier transport characteristics. *Pharm Res* **12,** 129–133.

Denissen JF, Grabowski BA *et al* (1997). Metabolism and disposition of the HIV-1 protease inhibitor ritonavir (ABT-538) in rats, dogs, and humans. *Drug Metab Disp* **25:** 489–501.

Dudley MN (1995). Clinical pharmacokinetics of nucleoside antiretroviral agents. *J Infect Dis* **171:** S99–112.

Dykstra KH, Arya A *et al* (1993). Microdialysis study of zidovudine (AZT) transport in rat brain. *J Pharm Exp Ther* **267:** 1227–1236.

Fenstermacher JD (1989). Pharmacology of the blood-brain barrier. In *Implications of the Blood–Brain Barrier and Its Manipulation*. Neuwelt EA (ed): Plenum Medical Book Co: New York, pp. 137–155.

Fenstermacher JD, Blasberg RG *et al* (1981). Methods for quantifying the transport of drugs across brain barrier systems. *Pharmacology and Therapeutics* **14:** 217–248.

Fenstermacher JD, Rall DP *et al* (1970). Ventriculocisternal perfusion as a technique for analysis of brain capillary permeability and extra-cellular transport. In: *Capillary Permeability*. Crone C, Lassen NA (ed): Academic Press; New York, pp. 484–490.

Fink DJ, DeLuca NA *et al* (1996). Gene transfer to neurons using herpes simplex virus-based vectors. *Ann Rev Neurosci* **19:** 265–287.

Fishman RA (1980). Cerebrospinal Fluid in Diseases of the Nervous System. W.B. Saunders Co: Philadelphia.

Flexner C, Hendrix C (1997). Pharmacology of antiretroviral agents. In *AIDS: Biology, Diagnosis, Treatment and Prevention*. DeVita VT, Hellman S, Roxenberg SA (ed): Lippincott-Raven: Philadelphia, pp. 479–493.

Galinsky RE, Hoesterey BL *et al* (1990). Brain and cerebrospinal fluid uptake of zidovudine (AZT) in rats after intravenous injection. *Life Sci* **47:** 781–788.

Gallo JM (1991). Pharmacokinetic models for anticancer and antiviral drugs following administrations as novel drug delivery systems. In *Advanced Methods of Pharmacokinetic and Pharmacodynamic Systems Analysis*. D'Argenio DZ (ed): Plenum Press: New York, pp. 21–36.

Gallo JM (1994). Delivery of anti-HIV nucleosides to the central nervous system. *Advanced Drug Deliv Rev* **14:** 299–309.

Ghersi-Egea JF, Finnegan W, *et al.* (1996). Rapid distribution of intraventricularly administered sucrose into cerebrospinal fluid cisterns via subarachnoid velae in rat. *Neuroscience,* **75,** 1271–1288.

Greenwald RB (1997). Drug delivery systems: anticancer prodrugs and their polymeric conjugates. *Exp Opin Ther Patents* **7:** 601–609.

Greitz D (1993). Cerebrospinal fluid circulation and associated intracranial dynamics. *Acta Radiol* **34** (Suppl): 1–23.

Iversen PL, Copple BL *et al* (1995). Pharmacology and toxicology of phosphorothioate oligonucleotides in the mouse, rat, monkey and man. *Toxicol Letters* **82/83:** 425–430.

Kang Y-S, Boado RJ *et al* (1995). Pharmacokinetics and organ clearance of a 3′-biotinylated, internally [^{32}P]-labeled phosphodiester oligonucleotide coupled to a neutral avidin/monoclonal antibody conjugate. *Drug Metab Disp* **23:** 55–59.

Kessler JA, Fenstermacher JD *et al* (1976). Spinal subarachnoid perfusion of rhesus monkeys. *Am J Physiol* **230:** 614–618.

Kimberlin DW, Spector SA *et al* (1995). Assays for antiviral drug resistance. *Antiviral Res* **26:** 403–413.

Kuhl DE, Alavi A *et al* (1980). Local cerebral blood volume in head-injured patients. *J Neurosurg* **52:** 309–320.

Levin VA, Gilboe DD (1970). Blood volume, hematocrit and pressure relationship in the isolated perfused dog brain. *Stroke* **1:** 270–277.

Levy RM, Ward S, *et al.* (1997). Alternative delivery systems for antiviral nucleosides and antisense oligonucleotides to the brain. *J Neurovirol,* **3,** S74–S75.

Lin JH, Chiba M *et al* (1996). Species differences in the pharmacokinetics and metabolism of indinavir, a potent human immunodeficiency virus protease inhibitor. *Drug Metab Disp* 1111–1120.

Lu D, Raizada MK (1995). Delivery of angiotensin II type 1 receptor antisense inhibits angiotensin action in neurons from hypertensive rat brain. *Proc Natl Acad Sci USA* **92:** 2914–2918.

Masereeuw R, Jaehde U *et al* (1994). *In vitro* and *in vivo* transport of zidovudine (AZT) across the blood brain barrier and the effect of transport inhibitors. *Pharm Res* **11:** 324–330.

McCarthy MM, Nielsen DA *et al* (1995). Antisense oligonucleotide inhibition of tryptophan hydroxylase activity in mouse brain. *Regulatory Peptides* **59:** 163–170.

McCarthy MM, Schlenker EH *et al* (1993). Enduring consequences of neonatal treatment with antisense oligodeoxynucleotides to estrogen receptor messenger ribonucleic acid on sexual differentiation of rat brain. *Endocrinology* **133:** 433–439.

Milhorat TH (1975). The third circulation revisited. *J Neurosurg* **42:** 628–645.

Morgan ME, Singhal D *et al* (1996). Quantitative assessment of blood-brain barrier damage during microdialysis. *J Pharmacol Exp Ther* **277:** 1167–1176.

Morrison PF, Laske DW *et al* (1994). High flow microinfusion: tissue penetration and pharmacodynamics. *Am J Physiol* **266:** R292–305.

Nakagawa H, Groothuis DR *et al* (1988). Dexamethasone effects on vascular volume and tissue hematocrit in experimental RG-2 gliomas and adjacent brain. *J Neurooncol* **6:** 157–168.

Nau R, Zysk G *et al* (1993). Pharmacokinetic quantification of the exchange of drugs between blood and cerebrospinal fluid in man. *Europ J Clin Pharmacol* **45,** 469–475.

Ohno K, Pettigrew KD *et al* (1978). Lower limits of cerebrovascular permeability to nonelectrolytes in the conscious rat. *Am J Physiol* **235:** H299–H307.

Oldendorf WH (1970). Measurement of brain uptake of radiolabeled substances using a tritiated water internal standard. *Brain Res* **24:** 372–376.

Parsons LH, Justice JB (1994). Quantitative approaches to *in vivo* brain microdialysis. *Critical Rev Neurobiol* **8:** 189–220.

Patlak CS, Fenstermacher JD (1975). Measurements of dog blood-brain transfer constants by ventriculocisternal perfusion. *Am J Physiol* **229:** 877–884.

Patlak CS, Blasberg RG *et al* (1983). Graphical evaluation of blood-to-brain transfer constants from multiple-time uptake data. *J Cereb Blood Flow Metab* **3:** 1–7.

Rapoport SI (1976). *Blood-Brain Barrier in Physiology and Medicine*. Raven Press; New York.

Rapoport SI, Fitzhugh R *et al* (1982). Drug entry into and distribution within brain and cerebrospinal fluid: [^{14}C]urea pharmacokinetics. *Am J Physiol* **242:** R339–R348.

Rapoport SI (1983). Passage of proteins from blood to cerebrospinal fluid. Model for transfer by pores and vesicles. In *Neurobiology of Cerebrospinal Fluid*. Wood JH (ed): Plenum Press: New York, pp. 233–246.

Renkin EM (1959). Transport of potassium-42 from blood to tissue in isolated mammalian skeletal muscle. *Am J Physiol* **197:** 1205–1210.

Robinson PJ, Rapoport SI (1990). Model for drug uptake by brain tumors: effect of osmotic treatment and of diffusion in brain. *J Cereb Blood Flow Metab* **10:** 153–161.

Rosenberg GA, Kyner WT *et al* (1980). Bulk flow of brain interstitial fluid under normal and hyperosmolar conditions. *Am J Physiol* **238:** F42–F49.

Saijo Y, Perlaky L *et al* (1994). Pharmacokinetics, tissue distribution, and stability of antisense oligonucleotide phosphorothioate ISIS 3466 in mice. *Oncol Res* **6:** 243–249.

Sakai F, Nakazawa K *et al* (1985). Regional cerebral blood volume and hematocrit measured in normal human volunteers by single-photon emission computed tomography. *J Cereb Blood Flow Metab* **5:** 207–213.

Sakai RR, He PF *et al* (1994). Intracerebroventricular administration of AT1 receptor antisense oligonucleotides inhibits the behavioral actions of angiotensin II. *J Neurochem* **62:** 2053–2056.

Sakai RR, Ma LY *et al* (1995). Intracerebroventricular administration of angiotensin type 1 (AT1) receptor antisense oligonucleotides attenuate thirst in the rat. (*Regulatory Peptides* **59:** 183–192.

Silverstein H (1996). Poster Presentation. *International Conference on AIDS*. Vancouver, BC.

Spector R, Spector AZ *et al* (1977). Model for transport in the CNS. *Am J Physiol* **232:** R73–R79.

Spector R (1980). Thymidine transport in the CNS. *J Neurochem* **35:** 1092–1098.
Spector R (1982). Pharmacokinetics and metabolism of cytosine arabinoside in the central nervous system. *J Pharmacol Exp Ther* **222:** 1–6.
Spector R, Eells J (1984). Deoxynucleoside and vitamin transport into the central nervous system. *Fed Proc* **43:** 196–200.
Spector R (1985a). Thymidine transport and metabolism in choroid plexus: effect of diazepam and thiopental. *J Pharmacol Exp Ther* **235:** 16–19.
Spector R (1985b). Uridine transport and metabolism in the central nervous system. *J Neurochem* **45:** 1411–1418.
Stahle L (1993). Microdialysis in pharmacokinetics. *Europ J Drug Metab Pharmacokin* **18:** 89–96.
Szklarczyk A, Kaczmarek L (1995). Antisense oligodeoxyribonucleotides: stability and distribution after intracerebral injection into rat brain. *J Neurosci Methods* **60:** 181–187.
Takasawa K, Terasaki T *et al* (1997). *In vivo* evidence for carrier-mediated efflux transport of 3′-azido-3′-deoxythymidine and 2′,3′-dideoxyinosine across the blood-brain barrier via a probenecid-sensitive transport system. *J Pharmacol Exp Ther* 369–375.
Terasaki T, Pardridge WM (1988). Restricted transport of 3′-azido-3′-deoxythymidine and dideoxynucleosides through the blood-brain barrier. *J Infect Dis* **158:** 630–632.
Walker WL, Cook J (1996). Drug delivery to brain tumors. *Bull Mathemat Biol* **58:** 1047–1074.
Wang L, Morin KW *et al* (1996). *In vivo* biodistribution, pharmacokinetic parameters, and brain uptake of 5-halo-y-methoxy (or ethoxy)-5,6-dihydro-3′-azido-3′-deoxythymidine diastereomers as potential prodrugs of 3′-azido-3′-deoxythymidine. *J Med Chem* 826–833.
Wang Y, Sawchuk RJ (1995). Zidovudine transport in the rabbit brain during intravenous and intracerebroventricular infusion. *J Pharm Sci* **84:** 871–876.
West ML, Fairlie DP (1995). Targeting HIV-1 protease: a test of drug-design methodologies. *Trend in Pharm Sci* **16:** 67–75.
Westergren I, Nystrom B *et al* (1995). Intracerebral dialysis and the blood brain barrier. *J Neurochem* **64,** 229–234.
Whitesell L, Geselowitz D *et al* (1993). Stability, clearance, and disposition of intraventricularly administered oligodeoxynucleotides: Implications for therapeutic application with the central nervous system. *Proc Natl Acad Sci USA* **90:** 4665–4669.
Wong SL, Van Belle K *et al* (1993). Distributional transport kinetics of zidovudine between plasma and brain extracellular fluid/cerebrospinal fluid in the rabbit: investigation of the inhibitory effect of probenecid utilizing microdialysis. *J Pharm Exp Ther* **264:** 899–909.
Wood JH (1980). *Neurobiology of Cerebrospinal Fluid*. Plenum Press: New York.
Wu D, Boado RJ *et al* (1996). Pharmacokinetics and blood-brain barrier transport of [^{3}H]-biotinylated phosphorothioate oligodeoxynucleotide conjugated to a vector-mediated drug delivery system. *J Pharmacol Exp Ther* **276:** 206–211.
Yaida Y, Nowak TS (1995). Distribution of phosphodiester and phosphorothioate oligonucleotides in rat brain after intraventricular and intrahippocampal administration determined by *in situ* hybridization. *Regulatory Peptides* **59:** 193–199.
Yasdanian M (1997). Poster Presentation. *Fourth Conference on Retroviruses and Opportunistic Infections, Washington, DC*.